Two-dimensional internal waves generated by a travelling oscillating cylinder

By T. N. STEVENSON AND N. H. THOMAS

Department of the Mechanics of Fluids, University of Manchester

Experiments are described in which an oscillating horizontal cylinder was moved through a density stratified fluid at Reynolds numbers of between 1 and 100 based on the diameter and mean velocity of the cylinder. The phase configurations of the internal waves which were generated are shown to compare very well with Lighthill's theory for waves in dispersive systems.

1. Introduction

The internal wave system present when a body oscillates in a stably stratified medium has been considered by Görtler (1943) and Mowbray & Rarity (1967a). The axisymmetric waves generated by a body moving vertically with a constant velocity have been described by Lighthill (1967) and Mowbray & Rarity (1967b), and the axisymmetric wave system around an oscillating moving body has been described by Stevenson (1969). The two-dimensional wave system around a cylinder moving with constant velocity was treated theoretically by Rarity (1967) and experimentally by Stevenson (1968). In all cases the experimental phase configuration of the internal waves compared reasonably well with the linear theory for small amplitude waves.

This note is concerned with the phase configuration of the two-dimensional waves which are generated in a stratified fluid when a cylinder moves with a constant velocity on which is superimposed an oscillation of known frequency. A circular cylinder was traversed with a velocity normal to its horizontal longitudinal axis so that its path made an angle with the horizontal. The waves due to the oscillation move through the steady wave system which is stationary relative to the cylinder. Schlieren pictures of the resulting wave patterns are compared with Lighthill's (1967) theory for dispersive waves.

2. Theoretical predictions

A co-ordinate system will be used with x horizontal and y vertical and positive upwards with the origin fixed in the body whose constant velocity relative to the undisturbed fluid is (U, V). If k_1 and k_2 are the wave-numbers in the x- and y-directions then the dispersion relation for short wavelength internal gravity waves takes the form (Stevenson 1968)

$$P(\omega, k_1, k_2) = \omega^2(k_1^2 + k_2^2) - \omega_0^2 k_1^2 = 0. \tag{1}$$

$\omega = (\omega_f + Uk_1 + Vk_2)$ is the frequency governing the direction in which energy is propagated, ω_f is the frequency of the oscillatory forcing effect and

$$\omega_0^2 = -(g/\rho_0)\,(d\rho_0/dy)$$

is the square of the Väisälä–Brunt frequency which will be considered constant. ρ_0 is the density of the undisturbed fluid and g is the acceleration due to gravity.

In order to plot the wave-number surfaces, (1) is written in the parametric form

$$\frac{W}{\omega_0}(k_1, k_2) = \frac{\pm \sin\theta - N}{\sin(\alpha - \theta)}\,(-\sin\theta, \cos\theta), \qquad (2)$$

where N is the frequency ratio ω_f/ω_0, α is the angle which the path of the body makes with the horizontal and $W = (U^2 + V^2)^{\frac{1}{2}}$ is the velocity of the body. Wave-number surfaces for $\alpha = 45°$ and $0°$ are presented in figures 1 and 2.
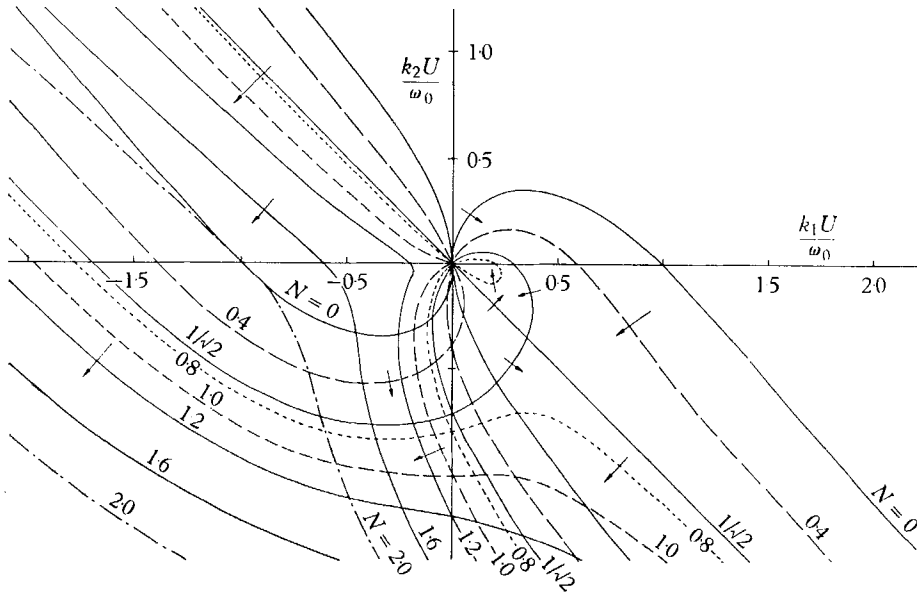

FIGURE 1. Wave-number surfaces for $\alpha = 45°$.

The wave-number curves for $\alpha = 90°$ are similar to those of the axisymmetric case presented by Stevenson (1969).

The regions in which energy is found are given by Lighthill's (1967) radiation condition. Thus the waves that exist in a certain direction from the forcing region are those with wave-numbers corresponding to points on the wave-number surface which have normals, drawn towards higher ω, which point in that particular direction. When $N > 1$ the wave-number surfaces do not pass through the origin, but when $N < 1$ the surfaces pass through the origin and their tangents are inclined at an angle ϕ to the k_2-axis where $\phi = \pm \sin^{-1} N$. In the first quadrant there are no waves in the steady case, $N = 0$, but waves are present if there is an oscillatory forcing term with N less than 1·0. For values of α close to $\frac{1}{2}\pi$ it can be shown that waves also occur in the first quadrant when N is between 1·0 and 1·1. When $N > 1$ waves will be found behind the body in a wedge-shaped region with
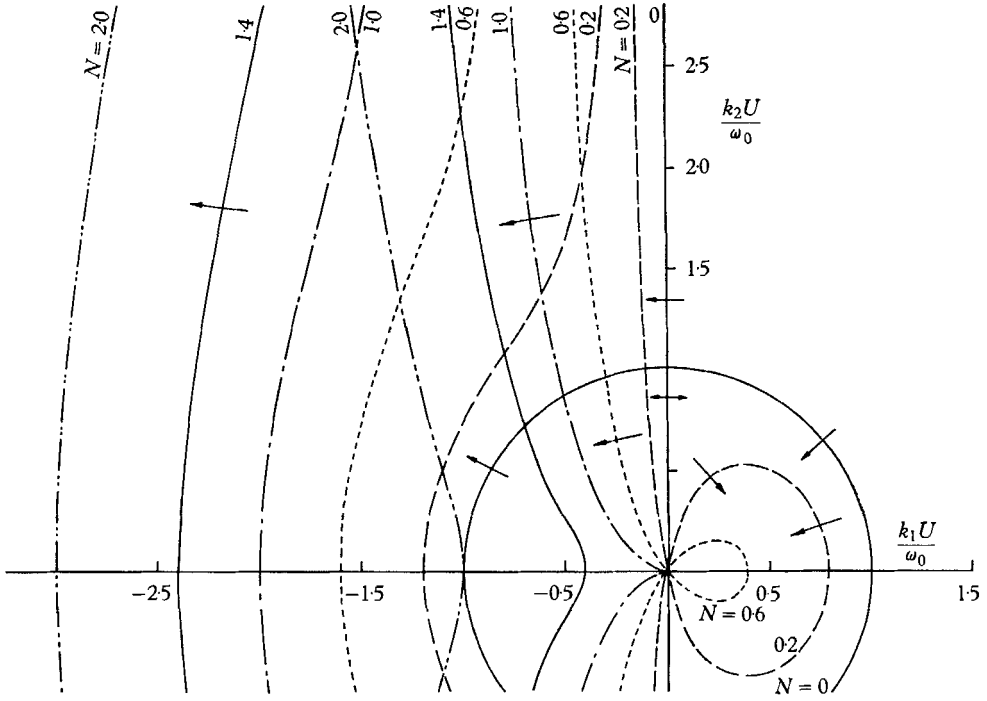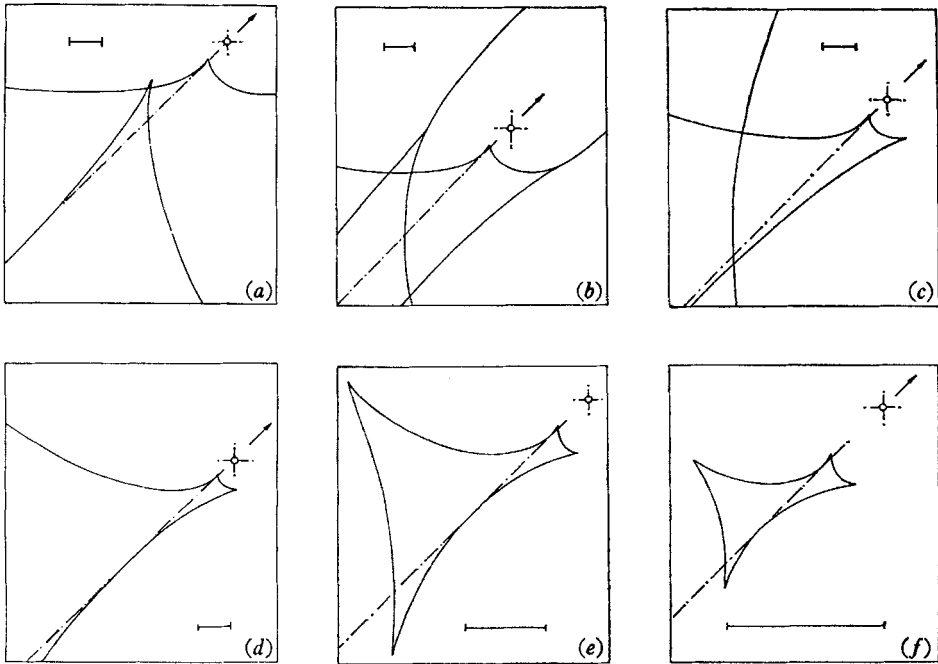
FIGURE 2. Wave-number surfaces for $\alpha = 0°$.

FIGURE 3. Phase configuration for $\alpha = 45°$ plotted as $y\omega_0/AU$ against $x\omega_0/AU$ when N is equal to (a) 0·6, (b) $1/\sqrt{2}$, (c) 0·8. (d) 1·0, (e) 1·4 and (f) 2·0. The scale marks are of length unity.

an included angle which decreases as N is increased. In general there are three main régimes which are (a) $N < \sin \alpha$, (b) $1 > N > \sin \alpha$ and (c) $N > 1$. However, régime (a) is absent in the limiting case when $\alpha = 0°$ and régime (b) is absent when $\alpha = 90°$.

Lighthill (1967) shows that the locus of points of constant phase is given by $A\nabla P/(\mathbf{k} . \nabla P)$ where $\mathbf{k}$ is the wave-number vector, ∇ is the gradient operator in $\mathbf{k}$ space and A is a constant. The phase configuration evaluated from (1) is

$$(x, y)\,\omega_0/A\,W = B\cosec(\alpha - \theta)\,(B\cos^2\theta + \cos\alpha, B\sin\theta\cos\theta + \sin\alpha), \qquad (3)$$

where
$$B = \sin(\alpha - \theta)/(\pm\sin\theta - N).$$

Figure 3 shows the phase configurations when $\alpha = 45°$ for several frequency ratios and the three régimes are seen in figure 3 (a), (c) and (e) corresponding to $N < \sin\alpha$, $1 > N > \sin\alpha$ and $N > 1$. The change from one régime to another is seen in figure 3 (b) for which $N = \sin\alpha$ and in figure 3 (d) for which $N = 1$. Equation (3) has been used to calculate the wave patterns which are shown on the right-hand side of figures 6–9, plates 1–4. Only the first few waves of each family are shown.

3. The experiments

The water tank which was filled with a stratified salt solution with a constant density gradient and the trolley, on which different size cylinders could be mounted, were the same as those used to produce the steady wave system (Stevenson 1968). In the experiments the linear density distribution over the depth of the working section was close to the exponential distribution implied by the constant Väisälä–Brunt frequency assumed in the theory. An inhomogeneity with respect to ω_0 changes the wave pattern but the effects were small in the present experiments. A system of levers and pulleys and two small electric motors were used to move the trolley with a constant velocity on which was superimposed an oscillation of known frequency. A schlieren system developed by Mowbray (1966) was used to observe the resulting wave patterns and some photographs are shown in figures 6–10, plates 1–4. The vertical white line in the photographs is the cylinder supports and we are looking along the axis of the cylinder.

When $\alpha = 0°$ the wave pattern corresponding to that in figure 3 (b) occurs when $N = 0$ and equation (3) then reduces to $(x, y)\,\omega_0/A\,W = (-\sin\theta, \cos\theta)$. In this case the waves consist of a series of semi-circles occupying the second and third quadrants and centred on the origin. When $\alpha = N = 0$ the group velocity is given by $Vg = \pm W\cos\theta$. It is subject to the radiation condition and is in a direction making an angle θ with the horizontal. Thus, if a body moves horizontally with constant velocity from a starting point S, energy will be found in a circle passing through the body and through the point S such that its centre is on the path of the body. As an example, in figure 8 (d), plate 3, some waves of this type are shown by the dashed lines. (Only the first few waves of the system are shown.) The experiments with a 0·24 cm diameter cylinder show a semi-circular wave pattern within a circular region passing through the body and through the point from which the body started. However, the waves continue outside this region. Possibly this is due to the waves created by the impulsive start or to the finite size of the

disturbance. A smaller cylinder 0·1 cm in diameter and 10 cm long was traversed horizontally with a velocity of 0·55 cm/s and the improved result is shown in figure 10, plate 4. The cylinder was moving from right to left and the three photographs show the way in which the wave pattern changes with time. The starting point can be seen by a mark one-eighth of the picture width from the right-hand side of each photograph.
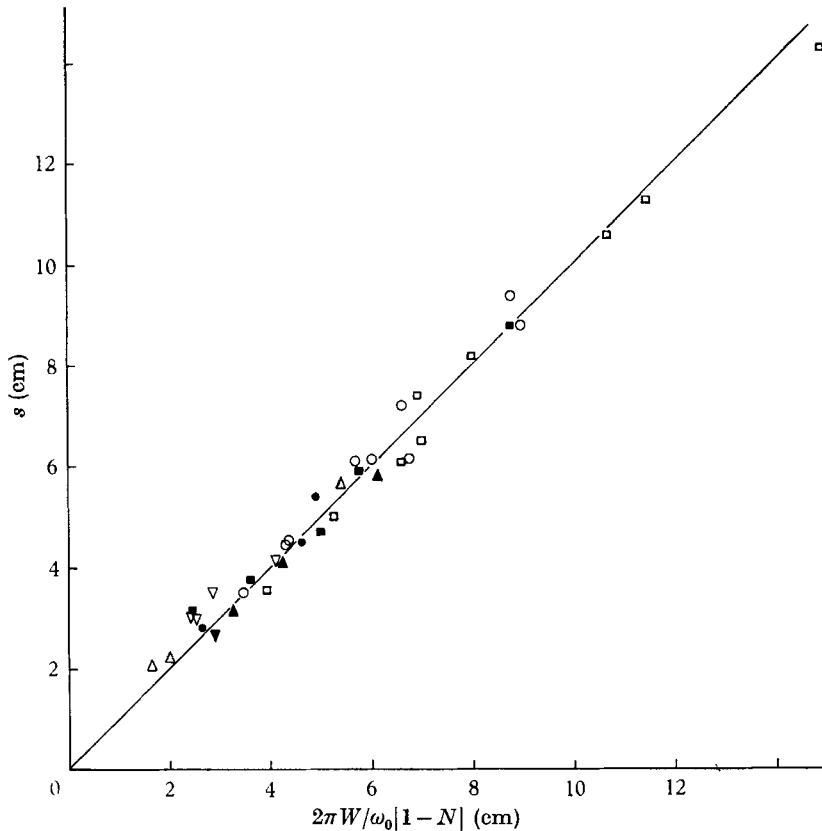

FIGURE 4. The distances between successive waves crossing the path of the cylinder when the velocity–frequency ratio is varied. The straight line is from the theory. The experimental points when $N < 1$ are represented by: $\square$, $\alpha = 45°$; $\bigcirc$, $\alpha = 20°$; $\triangle$, $\alpha = 10°$; $\triangledown$, $\alpha = 0°$; and when $N > 1$ by: $\blacksquare$, $\alpha = 45°$; $\bullet$, $\alpha = 20°$; $\blacktriangle$, $\alpha = 10°$; $\blacktriangledown$, $\alpha = 0°$. Experimental points for the steady case $N = 0$ are not included in the figure.

The theoretical wave patterns calculated from (3) using the relevant values for α, N and ω compare very well with the photographs. For a particular α and frequency ratio, N, the wave spacing depends on the velcocity of the body and the Väisälä–Brunt frequency. The distance between the waves increases as the velocity of the body increases. This is illustrated clearly in figure 8 (a)–(d), plate 3, where the only difference between the two experiments is in the velocity of the cylinder which was 0·16 cm/s in one and 0·55 cm/s in the other. The same amplitude of oscillation was used for the two runs and the energy in the waves due to the oscillation is approximately the same in both cases whereas the first of the

steadily moving wave systems is much weaker than the second higher velocity traverse.

Along the path of the body the distance, s, between the waves is obtained from (3) by letting $\theta = \pm \frac{1}{2}\pi$ which corresponds to fluid oscillating with the Väisälä–Brunt frequency. The group velocity in this case is zero and the wave spacing is given by
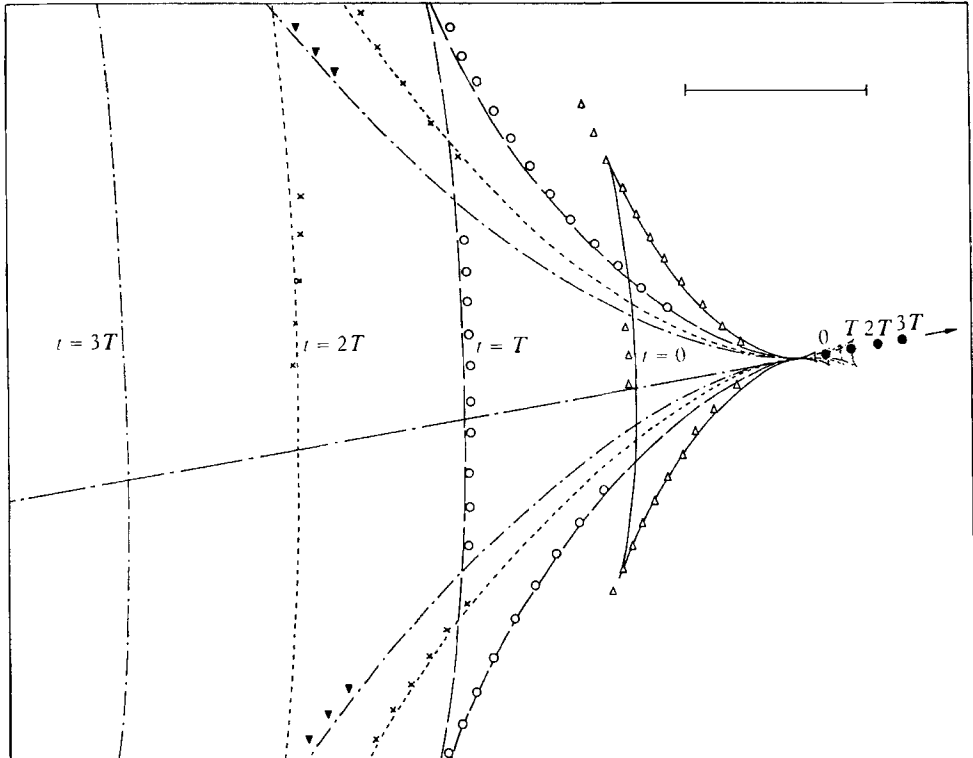
$$s = |2\pi W/\omega_0(N \pm 1)|,$$

FIGURE 5. The growth of a wave shown with time intervals corresponding to T, the period of oscillation of the cylinder. The position of the cylinder at each time is also shown. The axes are fixed relative to the unperturbed fluid and the scale mark is of length 5 cm. The lines are from the theory and the points are from the experiments. ($\alpha = 10°$, $W = 0.151$ cm/s, $T = 68$ s and $N = 1.15$.)

which is independent of α. For each value of N there are two points at which the waves with the same phase cross the path of the body (see figure 3). The distance between the waves with the larger spacing along the path of the body can be measured from the photographs and the results of this are shown in figure 4. The agreement between theory and experiment is good. Stevenson (1968) showed that the results for $N = 0$ also plot onto the same straight line.

The phase configuration of a wave remains geometrically similar, but changes in size so that the points with horizontal tangents remain in the same horizontal plane because at these points the phase velocity is zero. It is not possible to measure the phase velocity directly from the experiments although the velocity

at which a particular wave crest moves along a line from the body may be measured.

Theoretically this velocity is given by

$$V_m = \frac{W \sin\theta \sin(\alpha - \theta)}{(\pm\sin\theta - N)\sin(\phi - \theta)}, \quad \text{where} \quad \phi = \tan^{-1}(y/x).$$

Along the path of the body where $\theta = \pm\frac{1}{2}\pi$ this reduces to $V_m = W(1 \pm N)^{-1}$. This velocity is used together with the phase configuration to predict the growth of the wave shown in figure 5 which is for $\alpha = 10°$, $N = 1\cdot15$ and $W = 0\cdot151$ cm/s. The wave position is calculated at time intervals of T, where T is the period of oscillation of the cylinder, and it is plotted with axes stationary relative to the undisturbed fluid. Cine film of the experiment was projected onto this figure and the frame size was adjusted so that the scales were the same. The points on the figures show how a particular wave appeared at time intervals of T. Again the agreement is good. The theoretical waves in figure 5 could have been plotted directly using the phase configuration, the velocity of the body and the wave spacing along the path of the body.

4. Concusions

The conclusion is the same as that reached in the previous notes on internal waves, namely that the linearized theory predicts the phase configuration of the waves reasonably well.

REFERENCES

GÖRTLER, H. 1943 *Z. angew. Math. Mech.* **23**, 65.

LIGHTHILL, M. J. 1967 *J. Fluid Mech.* **27**, 725.

MOWBRAY, D. E. 1966 *J. Fluid Mech.* **27**, 595.

MOWBRAY, D. E. & RARITY, B. S. H. 1967a *J. Fluid Mech.* **28**, 1.

MOWBRAY, D. E. & RARITY, B. S. H. 1967b *J. Fluid Mech.* **30**, 489.

RARITY, B. S. H. 1967 *J. Fluid Mech.* **30**, 329.

STEVENSON, T. N. 1968 *J. Fluid Mech.* **33**, 715.

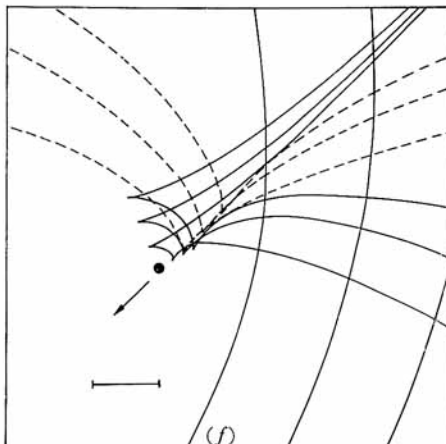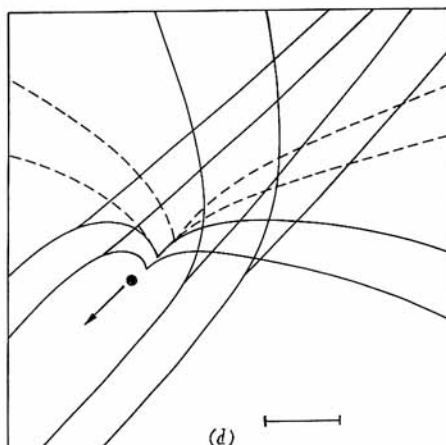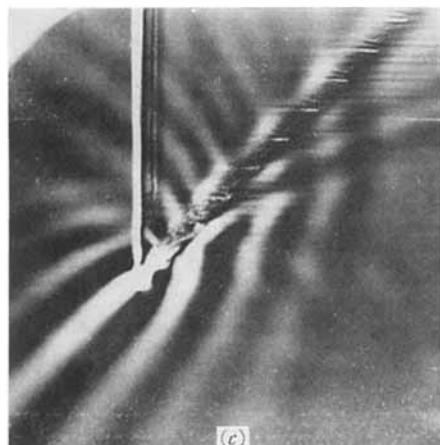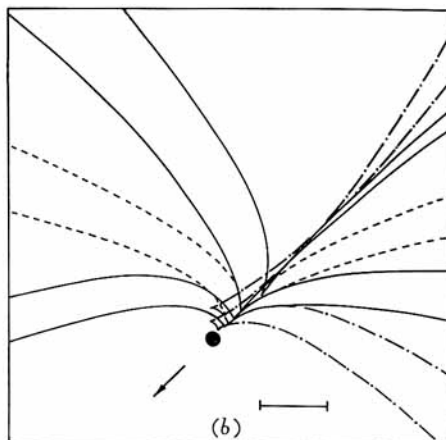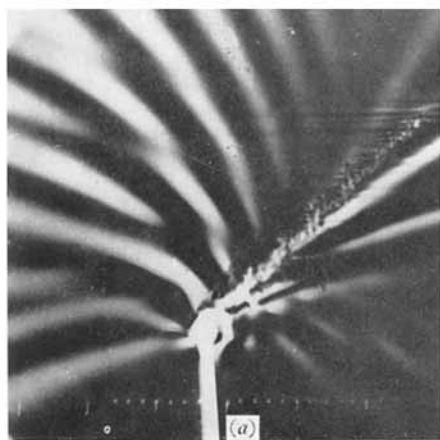STEVENSON, T. N. 1969 *J. Fluid Mech.* **35**, 219.

FIGURE 6. Experimental and theoretical internal wave patterns when $\alpha = 45°$. (a) and (b) $\omega_0 = 1·13$ rad/s, $W = 0·28$ cm/s, $N = 0·48$ for the $0·94$ cm diameter cylinder. (c) and (d) $\omega_0 = 1·06$ rad/s, $W = 0·35$ cm/s, $N = 0·707$ for the $0·24$ cm diameter cylinder. (e) and (f) $\omega_0 = 1·06$ rad/s, $W = 0·36$ cm/s, $N = 0·81$ for the $0·24$ cm diameter cylinder. The chain dotted lines are the first harmonics and the dashed lines are the steady waves. The scale marks represent a length of 5 cm.
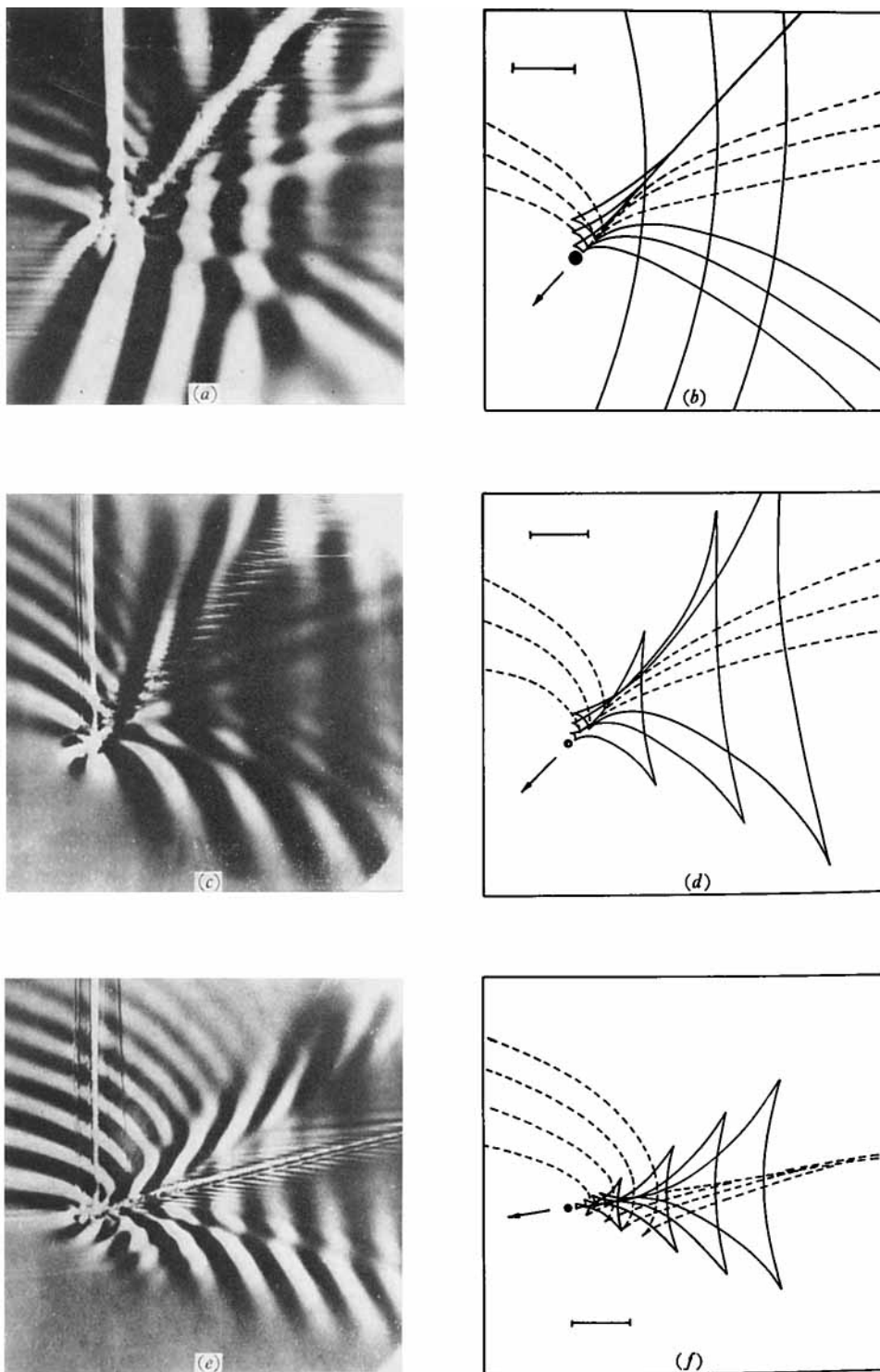
FIGURE 7. Experimental and theoretical wave patterns. The scale marks represent a length of 5 cm. (a) and (b) $\alpha = 45°$, $\omega_0 = 1·13$ rad/s, $W = 0·20$ cm/s and $N = 0·86$ for the 0·94 cm diameter cylinder. (c) and (d) $\alpha = 45°$, $\omega_0 = 1·06$ rad/s, $W = 0·27$ cm/s and $N = 1·18$ for the 0·24 cm diameter cylinder. (e) and (f) $\alpha = 10°$, $\omega_0 = 1·17$ rad/s, $W = 0·35$ cm/s and $N = 1·45$ for the 0·24 cm diameter cylinder.
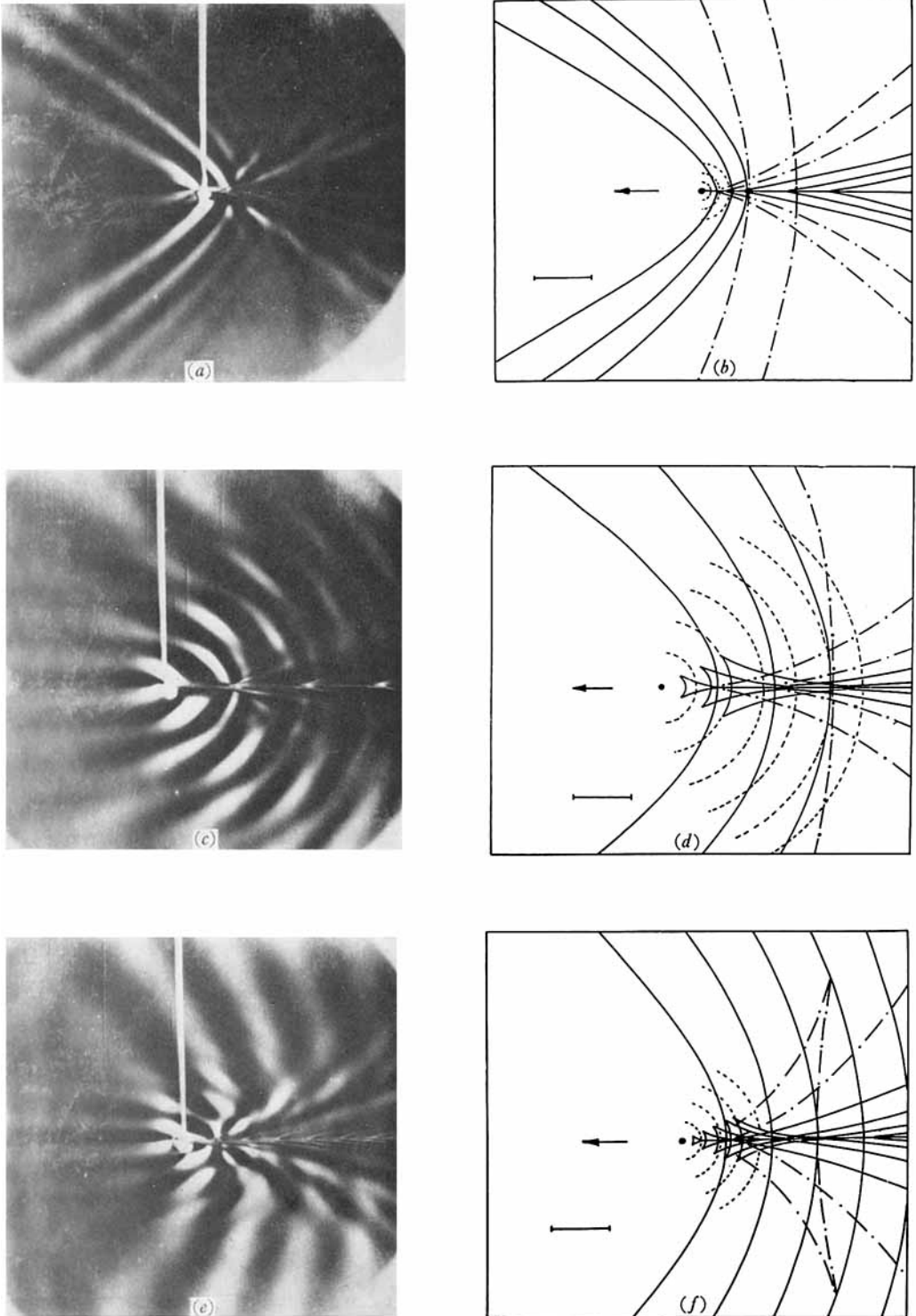
STEVENSON AND THOMAS

FIGURE 8. Experimental and theoretical wave patterns for the 0·24 cm diameter cylinder moving horizontally when $\omega_0 = 1·27$ rad/s. The scale marks represent a length of 5 cm. The dashed lines are the steady waves and the chain dotted lines are the first harmonics. (a) and (b) $W = 0·16$ cm/s and $N = 0·40$. (c) and (d) $W = 0·55$ cm/s and $N = 0·40$. (e) and (f) $W = 0·34$ cm/s and $N = 0·57$.
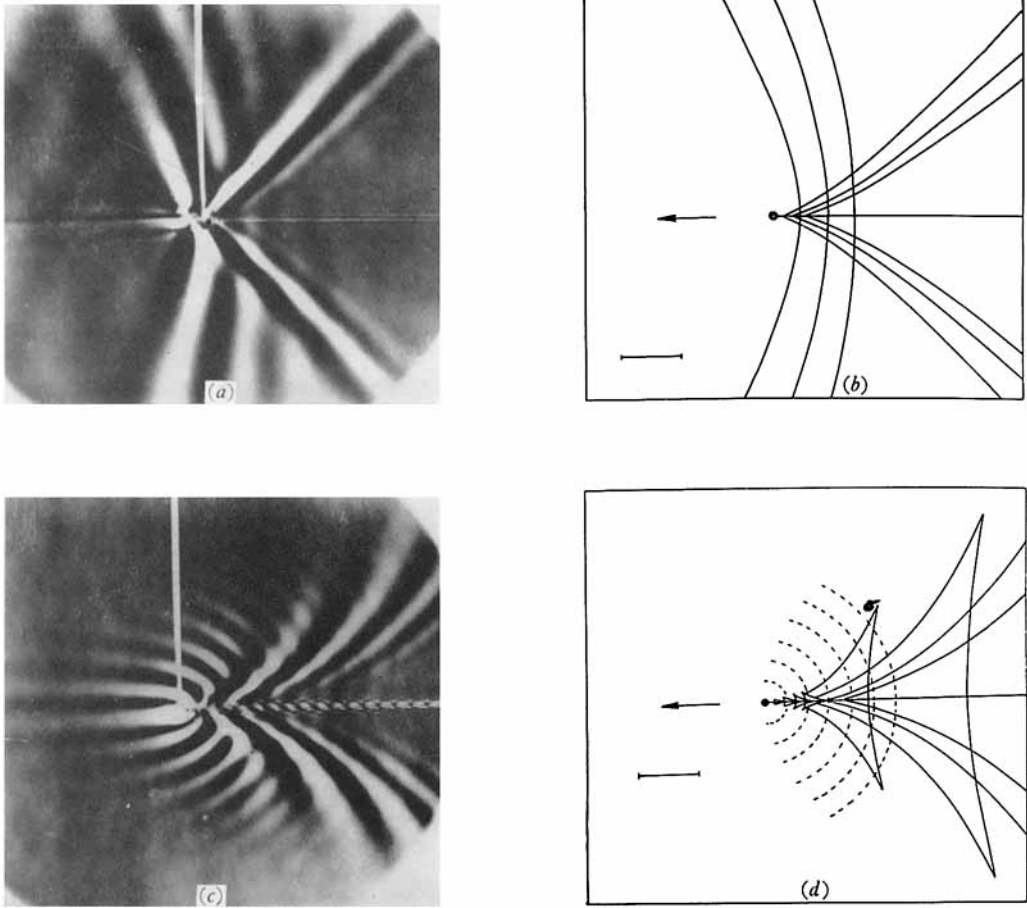
STEVENSON AND THOMAS

FIGURE 9. Experimental and theoretical wave patterns for the 0·24 cm diameter cylinder moving horizontally when $\omega_0 = 1\cdot27$ rad/s. The scale marks represent a length of 5 cm. (a) and (b) $W = 0\cdot086$ cm/s and $N = 0\cdot82$. (c) and (d) $W = 0\cdot36$ cm/s and $N = 1\cdot21$.
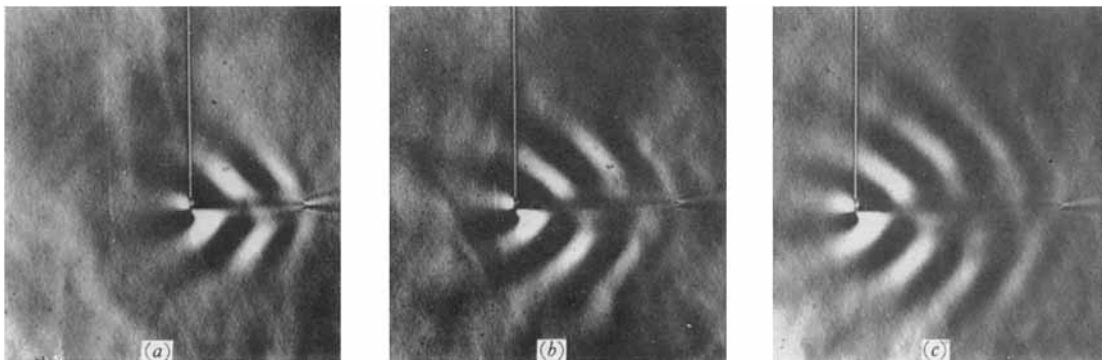

FIGURE 10. The development of a wave system when $\alpha = N = 0$ and $W = 0\cdot55$ cm/s for the 0·1 cm diameter cylinder.

STEVENSON AND THOMAS